

Effect of uncoupling protein-1 expression on 3T3-L1 adipocyte gene expression

Fatih S. Senocak^a, Yaguang Si^b, Colby Moya^a, William K. Russell^c, David H. Russell^c,
Kyongbum Lee^d, Arul Jayaraman^{a,*}

^a Artie McFerrin Department of Chemical Engineering, Texas A&M University, College Station, TX 77843-3122, United States

^b Department of Biology, Tufts University, Medford, MA 02155, United States

^c Department of Chemistry, Texas A&M University, College Station, TX 77843-3122, United States

^d Department of Chemical and Biological Engineering, Tufts University, Medford, MA 02155, United States

Received 31 July 2007; revised 1 November 2007; accepted 21 November 2007

Available online 3 December 2007

Edited by Berend Wieringa

Abstract The mitochondrial respiratory uncoupling protein 1 (UCP1) partially uncouples substrate oxidation and oxidative phosphorylation to promote the dissipation of cellular biochemical energy as heat in brown adipose tissue. We have recently shown that expression of UCP1 in 3T3-L1 white adipocytes reduces the accumulation of triglycerides. Here, we investigated the molecular basis underlying UCP1 expression in 3T3-L1 adipocytes. Gene expression data showed that forced UCP1 expression down-regulated several energy metabolism pathways; but ATP levels were constant. A metabolic flux analysis model was used to reflect the gene expression changes onto metabolic processes and concordance was observed in the down-regulation of energy consuming pathways. Our data suggest that adipocytes respond to long-term mitochondrial uncoupling by minimizing ATP utilization.

© 2007 Federation of European Biochemical Societies. Published by Elsevier B.V. All rights reserved.

Keywords: Uncoupling protein 1; Energy metabolism; Adipocytes

1. Introduction

Obesity is a chronic condition that develops due to excess accumulation of fats in adipose tissue and skeletal muscle, and increases the risk of many diseases including type 2 diabetes [1]. Hypertrophic expansion of white adipose tissue (WAT) results from the progressive accumulation of intracellular lipids (triglyceride, TG) [2]. Brown adipose tissue (BAT), although sharing many features with WAT, is not present in adult humans, and is specialized for adaptive thermogenesis [3] through expression of high levels of fatty acid oxidation enzymes and mitochondrial respiratory chain components. Of these, the mitochondrial respiratory uncoupling protein 1 (UCP1) is specifically enriched in BAT, while only minimally expressed in WAT [4]. In BAT, UCP1 dissipates the mitochondrial membrane potential by partially uncoupling substrate oxidation and oxidative phosphorylation, and promotes the dissipation of biochemical energy as heat [5]. Recent work

from our laboratory [6] has demonstrated that forced expression of UCP1 in 3T3-L1 adipocytes reduces accumulation of TG, which is consistent with the energy dissipative function of UCP1 reported by others [5,7]. Our data also suggested that the reduction in TG was due to down-regulation of fat synthesis, rather than an up-regulation of fatty acid oxidation.

In this study, we investigated the molecular basis of forced UCP1 expression in 3T3-L1 adipocytes. Microarrays were used to profile changes in gene expression and identify significantly altered metabolic genes/processes. A metabolic flux model was also used to determine fluxes through the energy metabolism pathways. Our data suggest that adipocytes respond to constitutive UCP1 expression by increasing protein stability and decreasing expression of genes encoding for energy-intensive processes, thereby minimizing energy utilization and maintaining constant ATP levels.

2. Materials and methods

2.1. Reagents and cell culture

3T3-L1 preadipocyte cells were obtained from ATCC (Manassas, VA). All tissue culture reagents including Dulbecco's modified Eagle's Medium (DMEM, 4.5 g/L glucose), calf serum (CS), fetal bovine serum (FBS) were purchased from Hyclone (Logan, UT). Human insulin and penicillin/streptomycin were purchased from Sigma (St. Louis, MO). Null-plasmid transfected 3T3-L1 preadipocytes (referred to as control adipocytes in this paper) and UCP1 expressing preadipocytes were cultured and differentiated into mature adipocytes as previously described [6]. Growth medium was replenished every other day through day 10 post-differentiation until cells were harvested for RNA isolation and/or mitochondrial isolation.

2.2. RNA extraction

Three independent cultures were used for extracting RNA from control and UCP1 expressing adipocytes. Total RNA was isolated from approximately 1×10^6 adipocytes at day 10 post-differentiation using the Nucleospin II RNA isolation kit from Clontech (Palo Alto, CA). RNA quality was determined on an Agilent 2100 Bioanalyzer (Agilent, CA), aliquoted, and stored at -80°C until further use.

2.3. Microarray analysis

RNA extracted from control and UCP1 expressing adipocytes were labeled and hybridized to Codelink™ mouse whole genome bioarrays (GE Healthcare Sciences, NJ) with ~36000 mouse gene targets. Labeling and hybridization experiments were performed at the Genomics core facility, Center for Environmental and Rural Health, Texas A&M University. Briefly, cDNA was synthesized from 2 µg of total RNA, purified, transcribed in vitro to yield biotin-labeled cRNA,

*Corresponding author. Fax: +1 979 845 6446.
E-mail address: arulj@tamu.edu (A. Jayaraman).

purified, and fragmented prior to hybridization using protocols provided by the manufacturer. Arrays were hybridized for 24 h, washed, and scanned on a Genepix 4000 microarray scanner (Molecular Devices, CA). Labeled cRNA from each control or UCPI adipocyte sample was hybridized to a single microarray (total of six microarrays). The expression data are available from the NCBI Gene Expression Omnibus (GEO, <http://www.ncbi.nlm.nih.gov/geo/>) and are accessible through GEO Series accession number GSE6643. The data were filtered to include only genes that were fully annotated and were present in all three replicate arrays. A one-way ANOVA filter was used to test each gene independently for a statistical difference in expression between the UCPI and control cells with a cutoff *P*-value of 0.05. The expression of nine genes was determined using quantitative RT. The mRNA sequence for each gene was retrieved from the Genbank database and gene specific primers designed for each transcript (Supplementary Table S3). RT-PCR was performed with ~50 ng of RNA using the Superscript II one-step RT-PCR kit (Invitrogen, CA) on a iycler real-time PCR machine (Bio-Rad, Hercules, CA). The cycle number at which the fluorescence in each amplification reaction increased beyond a threshold (in the exponential phase of amplification) was determined using the MyiQ software (Bio-Rad). Threshold cycle numbers for each gene were normalized to that of 18S rRNA (housekeeping gene) as described earlier [8]. All RT-PCR experiments were done in triplicate and data reported are means ± S.D.

2.4. Metabolite assays

As inputs for the flux calculation, the rates of uptake, output, or accumulation of 26 primary metabolites were measured by performing assays on cell lysates and spent medium samples. Cellular ATP was measured using a luminescence assay kit (Promega, Madison, WI) based on the ATP-dependent activity of luciferase. TG, glycerol, and free fatty acids (FFA) were measured using commercial assay kits as described previously [9]. Glucose, lactate, acetoacetate, and β-hydroxybutyrate were measured using enzymatic assays [9]. Ammonia and amino acids were quantified by HPLC [10]. All metabolite data were normalized by the corresponding DNA content of the corresponding cell sample.

2.5. Metabolic flux analysis

A stoichiometric model of adipocyte central carbon metabolism was constructed as described previously [9]. The model consisted of the following pathways: glycolysis, glycerogenesis, ketone body synthesis, lipogenesis, lipolysis, the malate cycle, the pentose phosphate pathway (PPP), and the TCA cycle (Supplementary Table S1). The same model was applied to both the control and UCPI expressing cells. As before, pathways were included (or omitted) based on physiological considerations as well as direct observations on the net rates of uptake or output of major metabolites. For example, fatty acid oxidation in UCPI expressing cells was assumed to be negligible (compared to lipogenesis and lipolysis) based on the observation that the oxygen utilization rate remained unchanged relative to control cells [6]. Intracellular fluxes were estimated by solving a constrained quadratic programming problem [11]:

$$\begin{aligned} \text{Minimize : } & \sum_k (v_k - v_k^{\text{obs}})^2 \quad \forall k \in \{\text{external fluxes}\} \\ \text{Subject to : } & \mathbf{S} \cdot \mathbf{v} = \mathbf{0} \quad (1) \\ & \mathbf{G} \cdot \mathbf{v} \leq \mathbf{0} \quad (2) \end{aligned}$$

where the objective is to minimize the sum squared error between experimentally observed and calculated exchange fluxes. Eq. (1) expresses the balances around intracellular metabolites using an $M \times N$ stoichiometric matrix \mathbf{S} and an $N \times 1$ steady-state flux distribution vector \mathbf{v} . Inequality (2) expresses constraints derived from the Gibbs free energy change form of the Second Law applied to pathways, as opposed to individual reactions.

2.6. Proteomic analysis

Protein expression levels in adipocytes expressing UCPI were determined using quantitative iTRAQ mass spectrometry (Applied Biosystems, CA). Adipocyte mitochondrial proteins were isolated using the protocol described by Pallotti and Lenaz [12], except that the initial cell lysis was performed in the tissue culture dish. Mitochondrial proteins from control or UCPI expressing adipocytes were digested with tryp-

sin and the peptides tagged with different isobaric mass tags. Equal amounts of tagged peptides from each sample were mixed together and separated on a strong cation exchange (SCX) column. Peptides from six SCX fractions were further separated using reverse phase chromatography on a 150 μm × 10 cm column (Vydac) using an LC-Packings autosampler and pumps (LC Packings, Sunnyvale, CA). A gradient of 2–40% acetonitrile was used to elute the peptides from the column at a flow rate of 1 μL/min. MALDI matrix (5 mg/mL α-cyano-4-hydroxycinnamic acid) was mixed with the column eluant through a “T” junction at 1.4 μL/min and spotted directly onto a MALDI sample plate using an LC-Packings Probot.

All MALDI-MS experiments were performed using a 4800 Proteomics Analyzer (Applied Biosystems, Foster City, CA). Data were acquired with the reflectron detector in positive mode (700–4500 Da, 1900 Da focus mass) using 800 laser shots (40 shots per sub-spectrum) with internal calibration. Collision induced dissociation tandem MS spectra were acquired using air at the medium pressure setting as the collision gas with 1 kV of collision energy. All MS and MS/MS data were searched against the Swiss-Prot protein sequence database using the GPS Explorer (Applied Biosystems) software.

3. Results

3.1. Changes in adipocyte gene expression upon UCPI expression

Approximately, 10% (3764 genes) of the ~36000 mouse genes represented on the Codelink whole genome bioarray passed the annotation, replicate, and ANOVA filters and were designated as significantly expressed in UCPI adipocytes relative to control adipocytes. The significantly activated or repressed genes were organized into 12 functional categories based on the gene ontology annotations provided along with the Codelink array. Fig. 1 shows the distribution of 1231 categorized genes over the different ontology categories. Four ontology categories – metabolism, signaling, transport, and transcriptional regulation – accounted for 60% of all significantly altered genes. Not surprisingly, metabolism genes were the single largest ontology category (239 genes or 19% of total). Genes involved in signaling, transport, and transcriptional regulation accounted for 16%, 14%, and 10%, respectively. Interestingly, apoptosis genes were also significantly expressed in UCPI expressing adipocytes. This included both pro- (e.g., caspase-1, Bcl associated death promoter) and anti- (e.g., B-cell leukemia/lymphoma 2, HSP40) apoptotic genes. Presumably, the forced UCPI expression resulted in an increase in apoptosis that was countered by the change in the expression of anti-apoptotic genes. However, the sequence of these events remains to be confirmed with further time-course experiments. Given the known role of UCPI in energy metabolism, we limit our discussion to describing alterations in the expression of metabolic genes.

3.2. Alterations in the expression of genes involved in metabolic processes upon UCPI expression

A majority of the metabolic genes demonstrating a significant change in expression upon UCPI expression were down-regulated (200 out of 239). This included genes involved in glycolysis (e.g., hexokinase, HK; phosphofructokinase, PFK; glyceraldehyde-3-phosphate dehydrogenase, GAPDH; aldolase), pentose phosphate pathway (hexose-6-phosphate dehydrogenase), glycogen metabolism (e.g., glycogen phosphorylase, glycogen synthase), citric acid cycle (e.g., citrate synthase, succinate dehydrogenase, fumarase, pyruvate dehydrogenase), oxidative phosphorylation (e.g., ATP synthases,

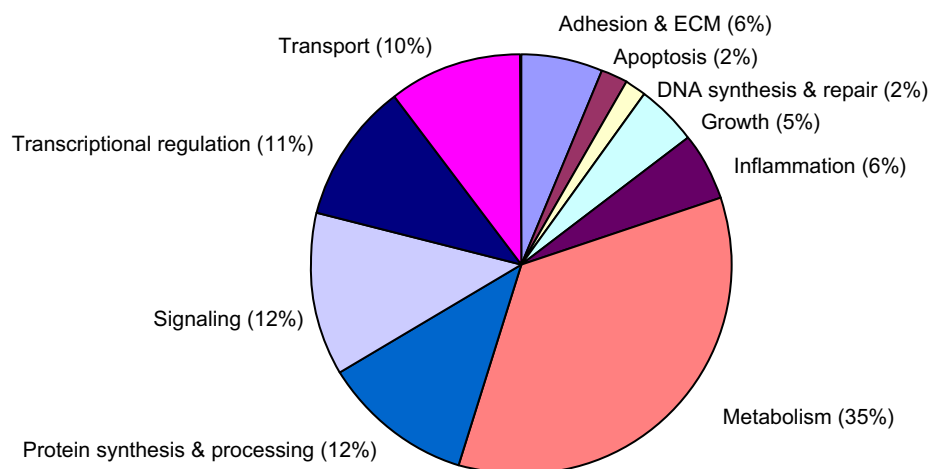


Fig. 1. Functional classification of statistically significant genes. Fully annotated genes which were determined to exhibit a statistically significant change in expression between control and UCPI adipocytes were classified based on their biological function using definitions in the Codelink array (GE Healthcare).

NADH dehydrogenases, cytochrome *c* oxidases), lipid catabolism (e.g., carnitine acyltransferase, acyl coA dehydrogenase), and lipid synthesis (e.g., fatty acid synthase, butyryl coA synthetase). A summary of changes in expression is shown in Table 1 and a complete list is included in Supplementary Table S2. For several of these processes (e.g., citric acid cycle), all significantly expressed genes were down-regulated. Pyruvate kinase (PK) was the only gene encoding for a glycolysis enzyme that was up-regulated. Interestingly, PK activity results in the net formation of ATP, while HK, PFK, and GAPDH all result in the phosphorylation of the substrate with either ATP (HK and PFK) or inorganic phosphate (GAPDH) as donors. UCPI expression in 3T3-L1 adipocytes up-regulated the expression of genes involved in glycerogenesis (e.g., phosphoenol pyruvate carboxykinase, glucose-6-phosphatase), detoxification (e.g., cytochrome P450 2E1, 4B1), and apolipoproteins (e.g., apolipoprotein D, apolipoprotein E receptor). Quantitative RT-PCR was used to corroborate the changes in the expression of several genes, including UCPI, fatty acid synthase, pyruvate kinase, and cytochrome P450 2E1 (Supplementary Table S3).

3.3. Estimation of metabolic flux in UCPI expressing adipocytes

Regulation of biochemical activity occurs at multiple levels, including by post-translational modification of enzymes and substrate availability. Therefore, we determined the flux through the different energy metabolism pathways at day 10 post-differentiation using a metabolic flux model and compared the changes in reaction fluxes with the corresponding gene expression data (Fig. 2). Significant changes were estimated for 12 of the 66 reactions included in the model. These were the reactions of glycolysis (Nos. 4 and 7, see Supplementary Table S1), lipid metabolism (Nos. 25–27), amino acid metabolism (Nos. 31, 35, and 48) and plasma exchange (Nos. 53, 55, and 66). These changes reflected an increase in the conversion of glycerone-phosphate into glyceraldehyde 3-phosphate (by 81%) and an increase in lactate output (by 168%). As a result, the net influx of pyruvate into the TCA cycle remained unchanged, but the supply of glycerone-phosphate for fatty acid esterification, and thus net TG synthesis, was significantly reduced (by 36%).

Table 1
Metabolic processes altered upon UCPI expression in 3T3-L1 adipocytes

Pathway or process	Number of genes
Glycolysis and related enzymes	15
Glycerolneogenesis and pentose phosphate pathway	3
Glycogen metabolism	4
Citric acid cycle	6
Oxidative phosphorylation	17
Amino acid, aromatic compound and purine metabolism	11
Lipid catabolism	17
Lipid biosynthesis	5
Uncoupling proteins	2
Cytochrome P450 enzymes	9
Apolipoproteins	6
Miscellaneous	24

Changes at the level of metabolite fluxes should lag transcriptional events, because of the many intervening layers of biochemical regulation. Therefore, we also obtained a second snapshot of the metabolic state at a later time point. On day 14, significant changes were estimated for 11 of the 60 reactions. These were the reactions of the PPP (Nos. 8 and 9), glycolysis (Nos. 2 and 7), lipid metabolism (Nos. 24–27), and alanine production (Nos. 35 and 53). The flux changes clustered essentially around two branch points: pyruvate and free fatty acid. Forced expression of UCPI decreased the PPP flux by 67%, while increasing lactate output by 410%. The net influx of pyruvate into the TCA cycle was unchanged, as were the TCA cycle fluxes. The PPP is a major producer of NADPH for de novo fatty acid synthesis. As expected, its down-regulation correlated with a 47% attenuation of acetyl-CoA export from the TCA cycle (via the citrate pool). A similar reduction (45%) was also estimated for FFA esterification into TG and the liberation of free glycerol by way of lipolysis.

Together, the metabolic flux data show that the PPP, fatty acid biosynthesis, and glyceroneogenesis were all significantly decreased whereas fermentation of pyruvate was increased by UCPI expression. Changes in PPP, fatty acid biosynthesis, and glyceroneogenesis were observed at the transcriptional level as well.

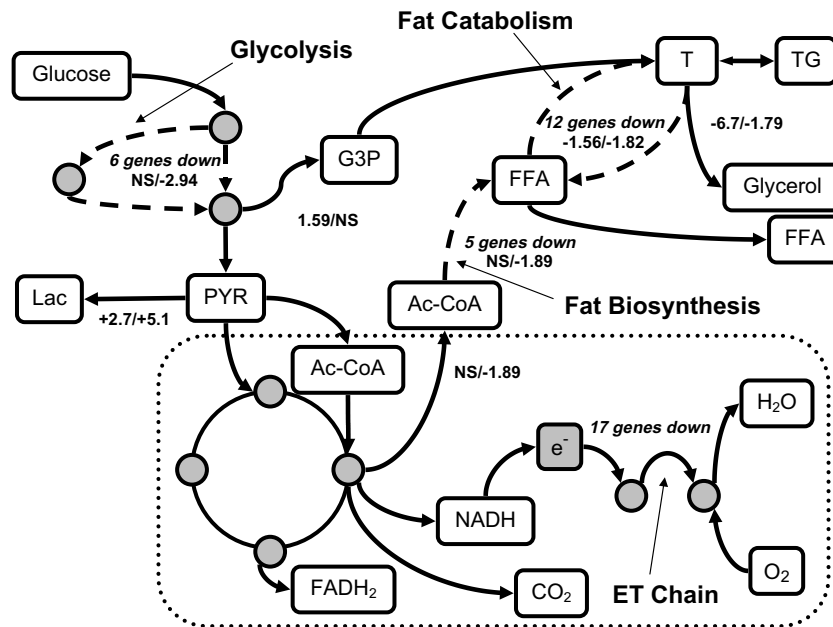


Fig. 2. Comparison of changes in gene expression and metabolite levels determined from metabolic flux analysis. Pathways significantly altered at both the metabolite level and gene expression are indicated by a dashed line. The fold-change in flux between UCPI and control adipocytes as well as the number of genes differentially expressed for each process is also indicated. In addition, pathways that were significantly altered either at the metabolite level or at the gene expression level only are also shown. Flux values at days 10 and 14 are given (day 10 value/day 14 value) and NS denotes statistically insignificant change in metabolite flux.

3.4. Lipid and ATP levels in UCPI expressing adipocytes

Microscopy images indicated that UCPI expressing adipocytes exhibited a characteristic morphology (round shape and

visible lipid droplets) (Fig. 3A and B) consistent with the known phenotype of differentiated 3T3-L1 adipocytes [13]. However, Oil-Red O staining showed that at day 10 post-induc-

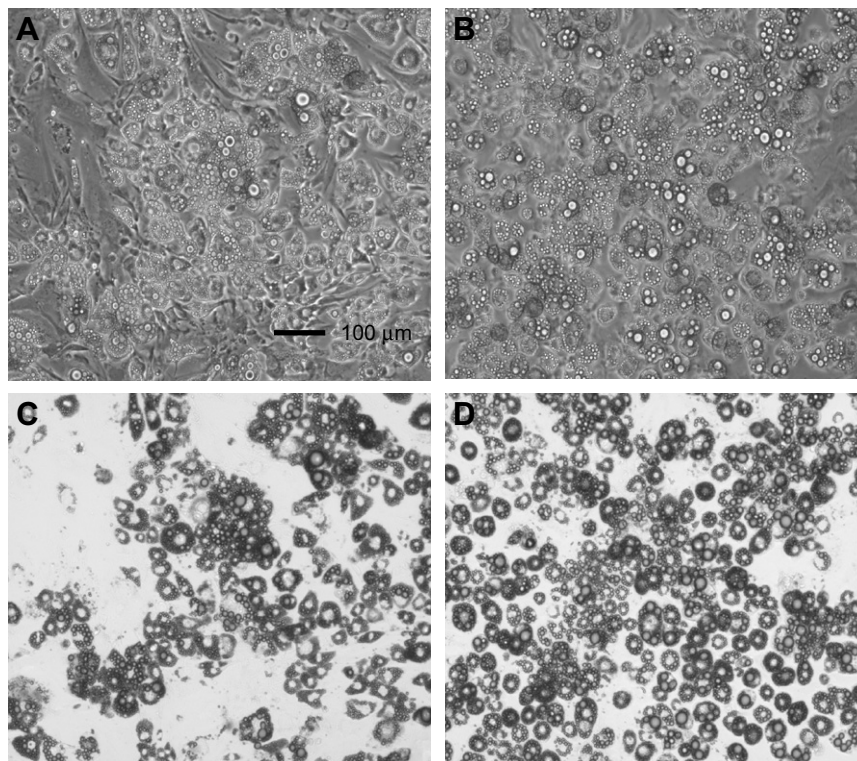


Fig. 3. Phase contrast (A and B) and Oil-Red O stained (C and D) images of UCPI expressing and control adipocytes at day 10 post-differentiation. Scale bar length is 100 μm.

tion, a noticeably smaller fraction of the culture contained visible lipid droplets (Fig. 3C and D). Our data show that the intracellular ATP levels at day 10 after differentiation are identical between the UCP1 expressing and control adipocytes (6.25 vs. 6.27 mMol-ATP/g-DNA). Together with the gene expression and metabolite flux data, these results indicate that while the overall energy metabolism flux is decreased, the ATP levels are maintained constant upon UCP1 expression.

4. Discussion

In this study, we used DNA microarrays and metabolic flux analysis to investigate at the molecular level the effect of constitutive UCP1 expression in 3T3-L1 adipocytes. UCP1 is a brown adipocyte protein that participates in non-shivering thermogenesis by lowering the mitochondrial membrane potential and promoting energy dissipation. Since UCP1 is only minimally expressed in white adipocytes, our interest was to determine the effect of exogenous UCP1 expression in white adipocyte gene expression and energy metabolism. We have previously shown that constitutive expression of UCP1 in 3T3-L1 adipocytes decreased lipid levels by decreasing fat synthesis rather than promoting fat oxidation. The gene expression data presented here indicate that UCP1 expression down-regulates the expression of several genes involved in energy metabolism (Table 1), including PPP, TCA cycle, lipid biosynthesis and catabolism. The observed changes in expression likely reflect cellular adaptation to long-term stress as the expression of UCP1 was constitutive (so as to mirror the conditions described in our prior work [6]), which can lead to decrease in the expression of genes involved in energy yielding and consuming processes.

Even with continuous expression of UCP1, ATP levels were similar between control and UCP1 adipocytes. This is surprising, as expression of UCP1 is expected to reduce the efficiency of oxidative phosphorylation, and decrease ATP levels in adipocytes. Although it is possible that compensatory mechanisms are present to utilize other energy sources (e.g., fatty acids) for maintaining ATP levels, our gene expression and metabolic flux data instead suggest down-regulation of lipid

catabolism pathways. The lack of direct correlation between UCP1 expression and lipid catabolism is also consistent with the observations of Enerbäck et al. [14] who showed that UCP1 knockout mice are not obese (i.e., as would be expected if UCP1 expression results in increased lipid catabolism). Based on the gene expression and metabolic flux changes, we hypothesize that the UCP1 expressing adipocytes maintained their ATP levels by minimizing ATP utilization (i.e., through the down-regulation of energy-dependent molecular processes). This is supported by the gene expression data (accessible through the GEO accession number GSE6643) showing that the expression of several signaling kinases that require ATP for function are down-regulated with UCP1 expression. The gene expression trends are also consistent with results at the level of protein expression. Analysis of 100 mitochondrial proteins, including those involved in electron transport chain ($n = 23$), TCA cycle ($n = 17$) and glycolysis ($n = 3$), in control and UCP1 expressing adipocytes by quantitative iTRAQ mass spectrometry [15] shows that 90 mitochondrial proteins are down-regulated in UCP1 adipocytes relative to control, with an average fold-change of 0.77 ± 0.18 .

The notion that adipocytes expressing UCP1 minimize energy expenditure can also be inferred from the changes in the expression of genes encoding for glycolytic enzymes. Our data (Table 1) show that pyruvate kinase, the only glycolytic enzyme that results in direct production of ATP (without the additional steps of electron transfer and oxidative phosphorylation), is also the only glycolysis gene up-regulated in UCP1 expressing adipocytes (1.18-fold; $P = 0.0015$). However, eight other glycolysis genes that either utilize ATP or do not produce ATP (e.g., hexokinase, aldolase) are down-regulated upon UCP1 expression. Our data suggest a scenario where UCP1 expression in 3T3-L1 adipocytes up-regulates reactions that generate ATP *directly*, as opposed to those that generate ATP by way of reducing potential for subsequent oxidative phosphorylation.

Our data show that the expression of 15 genes related to the ubiquitin proteasome system and other proteases (Table 2) were significantly down-regulated in UCP1 adipocytes. Since these proteases are involved in protein degradation and turnover, their down-regulation is expected to increase the overall

Table 2
Statistically significant changes in the expression of ubiquitin protease-related genes upon UCP1 expression in 3T3-L1 adipocytes

Gene	P-value	Expression ratio
Ubiquitin-activating enzyme E1, Chr Y 1 (Ube1y1)	0.046	-1.47
Proteasome (prosome, macropain) subunit, alpha type 1 (Psm1)	0.006	-1.74
Ariadne ubiquitin-conjugating enzyme E2 binding protein homolog 1 (Drosophila) (Arih1)	0.012	-1.43
Ubiquitin specific protease 27, X chromosome (Usp27x)	0.038	1.21
F-box and leucine-rich repeat protein 12 (Fbx12)	0.030	-1.23
Proteasome (prosome, macropain) subunit, alpha type 7 (Psm7)	0.029	-1.24
Ubiquitin specific protease 10 (Usp10)	0.039	-1.32
Proteasome (prosome, macropain) subunit, beta type 1 (Psm1)	0.023	-1.36
Ubiquitin specific protease 39 (Usp39)	0.017	-1.36
Ubiquitin-conjugating enzyme E2, J1 (Ube2j1)	0.011	-1.70
Ubiquitin protein ligase E3A (Ube3a), transcript variant 2	0.014	-1.41
Ubiquitin specific protease 3 (Usp3)	0.026	-1.32
Ubiquitin specific protease 3 (Usp3)	0.022	-1.34
General transcription factor III A (Gtf3a)	0.046	-1.29
Ubiquitin protein ligase Nedd-4 mRNA	0.004	-1.35
Adult male aorta and vein cDNA, RIKEN clone: A530064N14 product:unknown EST, full insert sequence	0.035	-1.47

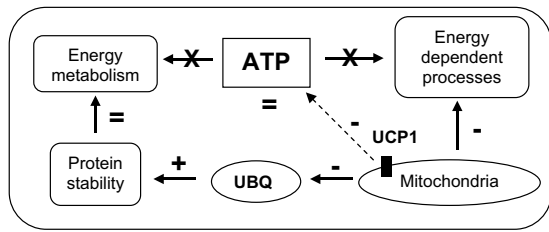


Fig. 4. Proposed model for effects of constitutive long-term expression of UCP1 in 3T3-L1 adipocytes.

protein half-life in adipocytes. Therefore, metabolic enzymes which would normally be degraded at a certain rate will be present and active for much longer in UCP1 expressing adipocytes. The long half-life of metabolic enzymes, in turn, can obviate the need for further *de novo* synthesis of these enzymes, thereby minimizing the energy requirement of the cell. This ATP utilization hypothesis is consistent with the earlier work of Buttgerit and Brand [16] that showed the existence of a distinct hierarchy of ATP consumption in concavalin A-treated thymocytes, with protein synthesis and DNA/RNA synthesis being most sensitive to ATP supply. Therefore, we propose that UCP1 expressing adipocytes down-regulate gene expression to maintain ATP levels constant. Interestingly, the study by Buttgerit and Brand found that the mitochondrial proton leak is among the least sensitive to ATP supply, which is also consistent with our observations (Supplementary Table S2).

The correspondence between changes in gene expression and enzyme activity was mixed. While some processes such as PPP and fat biosynthesis were decreased at both levels (as evidenced by decrease in the expression of multiple genes involved in these processes), others such as lactate production and oxidative phosphorylation were altered only at the metabolic flux or gene expression level, respectively. Our data suggests that multiple levels of regulation are utilized by 3T3-L1 adipocytes in the response to continuous mitochondrial uncoupling. Currently, it is not clear why certain processes are down-regulated at both the gene expression and metabolite levels while some others appear to be controlled only at one of the levels. One possibility is that only processes which *directly* yield ATP (e.g., glycolysis) are regulated at both the gene expression and metabolite flux levels (i.e., more tightly regulated).

Based on our data, we propose a model for changes in energy metabolism occurring upon forced expression of UCP1 in adipocytes (Fig. 4). In this model, the primary long-term response of adipocytes to constitutive mitochondrial uncoupling is to minimize ATP utilization through a combination of: (i) down-regulation of ATP-dependent molecular processes such as the expression of signaling kinases and (ii) increasing the half-life of metabolic enzymes through down-regulation of ubiquitin proteases, thereby minimizing the energy demands arising from transcription and translation. Based on these results, we hypothesize that ATP conservation is a manifestation of adaptation to long-term constitutive uncoupling. Current work in our laboratory focuses on comparing alterations in energy metabolism at the gene expression and metabolite levels by regulating UCP1 expression in adipocytes using doxycycline and the Tet-Off expression system [6].

Increasing energy expenditure in white adipocytes has been proposed as an alternative or complement to current obesity

therapies, which are generally aimed at reducing bodily nutrient intake. A number of *in vitro* studies have explored the induction of UCP1 through upstream activators as a means to enhance oxidative metabolism in white adipocytes [17–19]. Our findings also suggest that long-term UCP1 expression could attenuate adipocyte lipid accumulation, albeit through a mechanism that does not involve increased substrate oxidation. Prospectively, UCP1 and perhaps other mitochondrial membrane proton carriers could be developed as targets for pharmacological agents to treat obesity at the cellular level.

Acknowledgements: This study was supported by a Codelink microarray award to A.J. from the Center for Environmental and Rural Health at Texas A&M University through grant P30-ES09106 from the National Institute of Environmental Health Sciences and the Texas Engineering Experiment Station to A.J., the NIH (1 R21 DK67228-01) to K.L., and the NIH (1 S10 RR022378-01) and NSF (MRI-CHE 9629966) to D.H.R. is also acknowledged. F.S.S. was funded by a NSF Undergraduate program in biological and mathematical sciences through the Department of Biology at Texas A&M University.

Appendix A. Supplementary data

Supplementary data associated with this article can be found, in the online version, at doi:10.1016/j.febslet.2007.11.064.

References

- [1] Wickelgren, I. (1998) Obesity: how big a problem? *Science* 280, 1364–1367.
- [2] Yin, W. et al. (2004) NO-1886 decreases ectopic lipid deposition and protects pancreatic beta cells in diet-induced diabetic swine. *J. Endocrinol.* 180, 399–408.
- [3] Hansen, J. and Kristiansen, K. (2006) Regulatory circuits controlling white versus brown adipocyte differentiation. *Biochem. J.* 398, 153–168.
- [4] Nicholls, D.J. and Rial, E. (1999) A history of the first uncoupling protein, UCP1. *J. Bioenerg. Biomembr.* 31, 399–406.
- [5] Rousset, S., Alves-Guerra, M., Mozo, J., Miroux, B., Cassard-Doulcier, A., Bouillaud, F. and Ricquier, D. (2004) The biology of mitochondrial uncoupling proteins. *Diabetes* 53, S130–S135.
- [6] Si, Y., Palani, S., Jayaraman, A. and Lee, K. (2007) Effects of forced uncoupling protein 1 expression in 3T3-L1 cells on mitochondrial function and lipid metabolism. *J. Lipid Res.* 48, 826–836.
- [7] Kopecky, J., Rossmeisl, M., Flachs, P., Bardova, K. and Brauner, P. (2001) Mitochondrial uncoupling and lipid metabolism in adipocytes. *Biochem. Soc. Trans.* 29, 791–797.
- [8] Varvarovska, J. et al. (2004) Aspects of oxidative stress in children with Type 1 diabetes mellitus. *Biomed. Pharmacother.* 58, 539–545.
- [9] Si, Y., Yoon, J. and Lee, K. (2007) Flux profile and modularity analysis of time-dependent metabolic changes of *de novo* adipocyte formation. *Am. J. Physiol. Endocrinol. Metab.* 292, E1637–E1646.
- [10] Cohen, S. and De Antonis, K. (1994) Applications of amino acid derivatization with 6-aminoquinolyl-*N*-hydroxysuccinimidyl carbamate. Analysis of feed grains, intravenous solutions and glycoproteins. *J. Chromatogr. A* 661, 25–34.
- [11] Nolan, R.P., Fenley, A.P. and Lee, K. (2006) Identification of distributed metabolic objectives in the hypermetabolic liver by flux and energy balance analysis. *Metab. Eng.* 8, 30–45.
- [12] Pallotti, F. and Lenaz, G. (2001) Isolation and subfractionation of mitochondria from animal cells and tissue culture lines. *Meth. Cell Biol.* 65, 1–35.

- [13] Green, H. and Kehinde, O. (1975) An established preadipose cell line and its differentiation in culture. II. Factors affecting the adipose conversion. *Cell* 5, 19–27.
- [14] Enerbäck, S., Jacobsson, A., Simpson, E.M., Guerra, C., Yamashita, H., Harper, M.E. and Kozak, L.P. (1997) Mice lacking mitochondrial uncoupling protein are cold-sensitive but not obese. *Nature* 387, 90–94.
- [15] Wiese, S., Reidegeld, K.A., Meyer, H.E. and Warscheid, B. (2007) Protein labeling by iTRAQ: a new tool for quantitative mass spectrometry in proteome research. *Proteomics* 7, 340–350.
- [16] Buttgerit, F. and Brand, M. (1995) A hierarchy of ATP-consuming processes in mammalian cells. *Biochem. J.* 312, 163–167.
- [17] Kopecky, J., Clarke, G., Enerbäck, S., Spiegelman, B. and Kozak, L.P. (1995) Expression of the mitochondrial uncoupling protein gene from the aP2 gene promoter prevents genetic obesity. *J. Clin. Invest.* 96, 2914–2923.
- [18] Tiraby, C., Tavernier, G., Lefort, C., Larrouy, D., Bouillaud, F., Ricquier, D. and Langin, D. (2003) Acquirement of brown fat cell features by human white adipocytes. *J. Biol. Chem.* 278, 33370–33376.
- [19] Orci, L., Cook, W.S., Ravazzola, M., Wang, M.Y., Park, B.H., Montesano, R. and Unger, R.H. (2005) Rapid transformation of white adipocytes into fat-oxidizing machines. *Proc. Natl. Acad. Sci. USA* 101, 2058–2063.